Catena 119 (2014) 104–115

Contents lists available at ScienceDirect

Catena

journal homepage: www.elsevier.com/locate/catena

External supply of dust in the Taklamakan sand sea, Northwest China, reveals the dust-forming processes of the modern sand sea surface

Haibing Wang [a,*], Xiaopeng Jia [a], Kuan Li [b], Hongfang Wang [a]

[a] Key Laboratory of Desert and Desertification, Cold and Arid Regions Environmental and Engineering Research Institute, Chinese Academy of Sciences, 260 Donggang West Road, Lanzhou, Gansu Province 730000, PR China
[b] The Inner Mongolia Autonomous Region Land Investigation and Planning Institute, 11 Xueyuan West Road, Hohhot, Inner Mongolia Autonomous Region, PR China

ARTICLE INFO

Article history:
Received 13 March 2013
Received in revised form 24 March 2014
Accepted 26 March 2014
Available online 21 April 2014

Keywords:
Dust fallout
Particle size
Rare earth elements (REE)
Taklamakan sand sea
Dust formation processes

ABSTRACT

As one of the most important global dust sources, the sand sea and neighboring areas contain multiple types of surfaces that release dust, such as dry lakes and riverbeds, degraded oases, and Gobi surfaces. To understand the link between those active sources of dust and the dust formation process of the sand sea surface, we investigated dust fallout characteristics at a height of 3 m and rare earth element (REE) geochemistry of different landforms in the Taklamakan sand sea, which has frequent dust events. The seasonal fallout and concentrations of PM_{10} particles and monitoring results of their land surface concentrations show that the Taklamakan sand sea is surrounded by dust sources, and it's an important dust deposit area. The particle size characteristics of dust sediment suggest that the dust-conveying capacity of the Taklamakan sand sea is much stronger than that of the Gobi and degraded surfaces on the sand sea edge. During sand/dust storms, the fine dust fraction (<40 μm) can frequently recycle between the Taklamakan sand sea and the active dust emission areas. Chondrite-normalized REE patterns and Eu/Eu* vs. La_{CH}/Yb_{CH} and $(La/Yb)_{CH}$ vs. La_{CH} ratios of land surface PM_{10} fraction and dust PM_{10} fractions further suggest that there are two types of cycle processes for fine dust particles (<40 μm) between the Taklamakan sand sea and surrounding Gobi and degraded land. First, multiple large scale sand/dust storms have occurred between the Taklamakan sand sea and surrounding Gobi and degraded land over a long historical period. This has caused the fine fractions of land surface sediment to be strongly mixed over the entire Tarim Basin, and the geochemical characteristics of the land surface PM_{10} fractions have strong homogeneity. Second, a localized and seasonal sand/dust storms has released an abundance of fine dust particles from the surrounding area. These have been mixed and deposited in the Taklamakan sand sea under the dominant wind force, and most particulate material are probably also reworked by the wind as the sand saltates and the dunes migrate, resulting in REE concentrations of the dust PM_{10} fraction that are much higher than those from the surrounding areas.

1. Introduction

As the world's largest dust source, deserts and adjacent areas contain multiple types of sites and surfaces that release dust, such as dry lakes and riverbeds, degraded oases, and Gobi surfaces. However, the exact desert dust emission provenance and mechanism of production in desert areas at regional and global scales are often unclear and subject to debate. Some researchers contend that most dust originates from desert-margin dry lakes and river beds, degraded oases, and Gobi areas, because there are substantial amounts of dust particles from these sources. Dust particles have been deposited in those areas by past or present river/flood processes, and are released in modern sandstorms. (Prospero et al., 2002; Tegen, 2003; Tegen et al., 2002; Wang and Jia, 2012; Wang et al., 2008, 2011; Washington et al., 2006). Others believe that the dust originates from the sand sea surface. Although those surfaces have a lower dust content, they have the largest coverage (Zhang et al., 1996, 1998) and high production capacity of dust through eolian abrasion and other dust generating processes that remains a little-understood, as is known to be an important source for proximal coarse dust and desert margin loess deposits (Amit et al., 2014; Crouvi et al., 2008, 2012; Ta et al., 2013). These results ignore local dust cycle processes involving dust material, which frequently occur between the sand sea and neighboring dust-release point source(s) during windblown sand episodes. The results of more general analyses typically blur the contribution of sand sea surfaces or other dust sources to atmospheric dust, and cannot reveal mechanisms of dust formation and factors that determine its occurrence and regulation in desert areas. Therefore, exploring local dust cycle processes is important to discover insights of modern dust emission and formation processes in desert areas.

* Corresponding author. Tel.: +86 931 4967539.
E-mail address: HBWang@lzb.ac.cn (H. Wang).

http://dx.doi.org/10.1016/j.catena.2014.03.015
0341-8162/

The Taklamakan sand sea is in the center of the Tarim Basin of China. It is the world's second largest sand sea and a major source of global dust (Laurent et al., 2006; Zhang et al., 2003a, 2003b). The dust, which is associated with a global atmospheric circulation process, is part of the global-land-marine biogeochemical cycle process and is closely associated with global climate change (Gao and Washington, 2010a, 2010b). A large number of wind erosion observations in the field have suggested that the peripheral area of the Taklamakan sand sea has a high silty clay content and strong dust release capability (Li et al., 2008; Wang and Jia, 2012; Zhang et al., 2003a, 2003b). Those areas include bare dry river bed and lake surfaces, abandoned farmland, degraded diversifolia forest, activated scrub sand, mobile sand dunes, and Gobi surfaces. The content of silt-sized dust on the Taklamakan sand sea surface is relatively small, and its dust release capability is considered comparatively weak. However, modern Taklamakan sand sea surfaces still release dust at annual rates up to 65 Mt/yr (Laurent et al., 2006). Satellite remote sensing data (Shao et al., 2002, 2003) confirm large-scale dust events over the entire sand sea. Where do the dust materials originate for the Taklamakan sand sea surface? What is the connection between dust materials over the sand sea and peripheral areas? The Taklamakan sand sea was selected as the research site, with the objective to explore representative dust cycle processes in the desert area and reveal the sand sea surface dust formation mechanism.

Much scientific research has been conducted on the sand/dust source for the Taklamakan sand sea. The results suggest that fluvial processes have contributed greatly to formation of the sand sea. A large amount of silt sediment has been transported from surrounding mountains to the margins of oases and the Gobi desert by more than 60 rivers, and this is released in modern sandstorms. There have been large lakes in this desert in various periods of the late Quaternary, and these lacustrine sediments are also potentially direct sources of dust (Yang et al., 2006a, 2006b, 2011). Another potential onsite source of dust is glacial–fluvial deposits on the desert margins (Yang et al., 2002). At present, degraded land around the oases is expanding rapidly. The Tarim, Hotan, and other major rivers have disappeared, and downstream lakes have dried up because of earlier climate and human factors in more recent decades (Yang, 2001; Yang et al., 2012). All these degraded land surfaces have become major dust-release areas in the Taklamakan sand sea (Gao and Washington, 2009; Wang and Jia, 2012; Yang et al., 2006a, 2006b). Degradation of the oases has been continuous over the past 60 years, which had a direct relation with high-frequency sandstorms in Xinjiang in the 1950s (Ta and Dong, 2006). Few works have explored the link between the active sources of dust and its formation process for the Taklamakan sand sea surface.

Local dust cycle processes are difficult to observe quantitatively in field situations and to incorporate in numerical modeling. However, we can determine dust fallout characteristics near the surface for various regions during dust cycle processes via field observation. Sediments arising from dust fallout during sandstorms are a mixture of various-sized dust particles in certain proportions. However, the transmission pathway and the distance dust particles travel in the atmosphere are significantly influenced by the regional wind field and particle size (Patterson and Gillette, 1977; Pye, 1987; Sun et al., 2000, 2002). Generally, once dust particles <20 μm in diameter are released, they do not readily undergo dry settling because of gravity and turbulence effects. Rather, these particles can be suspended for long periods and be transported long distances. Dust particles >70 μm usually move by saltation and accumulate rapidly under gravitation. Therefore, particle size characteristics of dust fallout sediments and their rates of dust deposition are often widely used as dust source tracers (Wang et al., 2009; Xie et al., 2009). Rare earth elements (REE) are a series of typical immobile elements that do not readily fractionate during earth surface processes (Taylor and McLennan, 1985). This set of elements have been shown to be good tracers of dust sources and the transport process (Teresa et al., 2006; Yang et al., 2007; Zhang et al., 2009).

Therefore, in this paper, we reveal the local dust cycle process between the Taklamakan sand sea and surrounding Gobi and degraded land by analyzing the distribution of dust fallout, its sediment granularity and REE geochemical features. This gives insight to the modern dust formation mechanism of the sand sea surface.

2. Regional setting

The Taklamakan Desert is the largest in China (≈338,000 km^2) and is in the Tarim Basin, Xinjiang Province of Northwest China (Zhu et al., 1981). Drought, strong winds, and abundant sand material combine to cause strong windblown sand/dust activity and frequent dust events in the region. The landscape of the desert can be considered to have a ring belt distribution with the Taklamakan sand sea, the Gobi desert margin and degraded land, and oases between the edge of the Gobi desert and the degraded land (Fig. 1). The degraded land refers to the belt of vegetation and dry lake landforms affected by windblown sand and dust in the region around the sand sea, arising from both natural causes and human interference (Wang and Jia, 2012). There are significant spatial differences in landforms, vegetation type, and dominant wind flows (Fig. 2 and Table 1). The prevailing wind regime is strong northeasterly in the eastern part of the basin, which affects both the eastern and southeastern areas. Westerly, northwesterly and northerly airflows affect the western and northern parts of the basin. The highest 10-min mean maximum wind speed and direction during the monitoring periods were consistent with prevailing wind directions (Fig. 3). This figure shows that the wind energy in different areas clearly varies. Overall, from the eastern to western sand sea, northeasterly winds gradually weaken, whereas the influence of northwesterly wind gradually strengthens.

3. Sampling and analytic methods

The sample monitoring sites are shown in Fig. 1. These sites were selected according to the dominant wind direction and main surface landscape types in the study region. Dust traps were fixed at a height of 3–3.2 m on abandoned electric poles along the main road through the desert, over surfaces characterized as capacious and flat. Vegetation coverage and amounts of bare sand were variable. The dust traps were 26-cm long with an inlet diameter of 9 cm. Small glass beads were put into the traps to improve their dust collection efficiencies. Collection from the traps was done during two periods, the first lasting 36 days and the second 322 days (5 April–10 May 2010 and 11 May 2010–2 April 2011). When dust samples were collected, the dust traps were sealed, taken back to the laboratory and replaced by new traps. At the same time, we collected surface sediment samples using a shovel to scrape the top 2 cm from the ground surface over 40 cm^2 areas. Approximately 1 kg of surface material was collected and placed in plastic bags.

In the laboratory, samples from the land surface sediment were sieved to separate >63 μm and <63 μm fractions. The <63 μm fraction was heated with H_2O_2 to remove organic matter, and its particle size distribution was determined using a Mastersizer Laser (Malvern, Worcestershire, UK). The >63 μm fractions were determined by sieving. The PM_{10} and $PM_{40–63}$ fractions were calculated by weight percentage. For the collected dust samples, we first used deionized water to clean the dust traps and then collected the suspension with a pipette. The pipetted suspensions were then placed in airtight boxes and dried naturally, before measuring the total weight of dust gravimetrically using a scale with 0.01 g precision. Next, we measured the dust particle size composition characteristics using the laser particle size analyzer. The $PM_{40–63}$ component in dust was obtained using the combined screening method. For the <40 μm component, the samples were rinsed several times with deionized water, and the PM_{10} component was measured by filtering. Last, REE element concentrations were obtained for both $PM_{40–63}$ and PM_{10} components using inductively coupled plasma mass spectrometry, which was done at the analytical laboratory of the

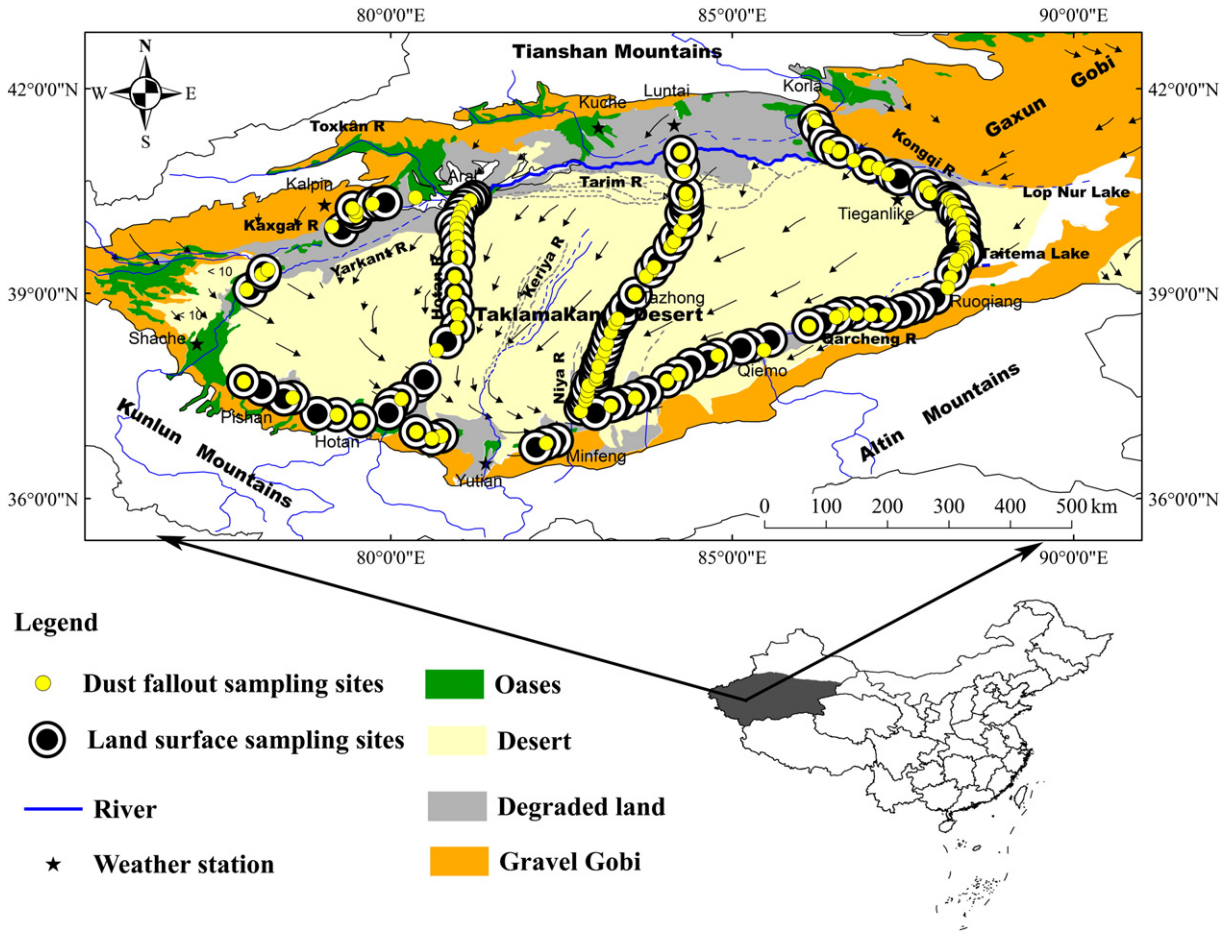

Fig. 1. Map of the study area showing the location of sampling sites.

Beijing Research Institute of Uranium Geology. The locations of the REE samples are shown in Fig. 4.

The PM_{10} fraction of dust existed in the loose material form is mainly attached to the sand surface and easily injected into the atmosphere by wind erosion in a desert area. Once PM_{10} particles are in the atmosphere, they normally exist as dust and are transported long distances. Thus, comparison of the rates of dust deposition and concentrations of PM_{10} particles and its concentrations of land surface sediments for different landscape surfaces reveals dust relationships between the Taklamakan sand sea and the surrounding Gobi desert and degraded lands. Comprehensive descriptions of curves of dust particle size composition content, accumulation, and grain size-standard deviation distribution are important means for recognizing particle size ranges of dust sediments that have undergone different modes of transport and have varying compositions (Wang et al., 2009; Xie et al., 2009). Furthermore, using contrasts in spatial distribution of the PM_{10} and PM_{40-63} fraction REE concentrations, plus chondrite-normalized REE patterns and REE ratios, allows testing of similarities and differences of spatial distribution. When combined with the dominant wind direction of the study region, this permits analysis of the function and significance of local dust processes between the Taklamakan sand sea and the surrounding Gobi and degraded land.

4. Results and discussion

4.1. Fallout and concentrations of PM_{10} particles and their surface concentrations

Even in a weaker wind energy environment, PM_{10} particles can be suspended in the atmosphere for long periods and be transported long distances. The spatial distribution of fallout and concentrations of PM_{10} particles for the whole motoring period and their surface concentrations are shown in Fig. 5. The results show that under the dominant wind direction, proportions of PM_{10} in sediment from the desert surface and dust are relatively low (mean values about 0.61% and 4.95%, respectively), but mean rates of dust deposition are high (mean values 1.46 g m^{-2} day^{-1}). The proportions increase from east to west and maximize in a southwestern desert airflow convergence area. In contrast, in the desert edge area, degraded land and Gobi surface areas, concentrations of the PM_{10} components are higher than in the Taklamakan sand sea along the dominant wind path. Mean concentrations of PM_{10} particles in the desert edge, degraded land and Gobi surface areas and dust are about 2.66% and 14.43%, respectively. In dust, the mean rates of accumulation are about 0.66 g m^{-2} day^{-1}. The results indicate that most of the dust emission sources are along the paths of prevailing wind directions and supply abundant aeolian dust materials to the Taklamakan sand sea surface.

This dust fallout monitoring confirmed the results of wind erosion observations. A large number of those observations in the field have suggested that the peripheral area of the Taklamakan sand sea has strong potential for wind erosion (Li et al., 2008; Wang and Jia, 2012; Zhang et al., 2003a, 2003b). This area includes bare surfaces, abandoned farmland, diversifolia forest, degraded land, activated scrub sand, mobile sand dunes, and Gobi surfaces. All these are characterized by a high silty clay content and strong dust release potential, and are along the path of the dominant wind. However, the content of silt dust at the sand sea surface is relatively low, and its dust release potential is weak. Visibly, the desert peripheral surface is the main dust source area, and the Taklamakan sand sea

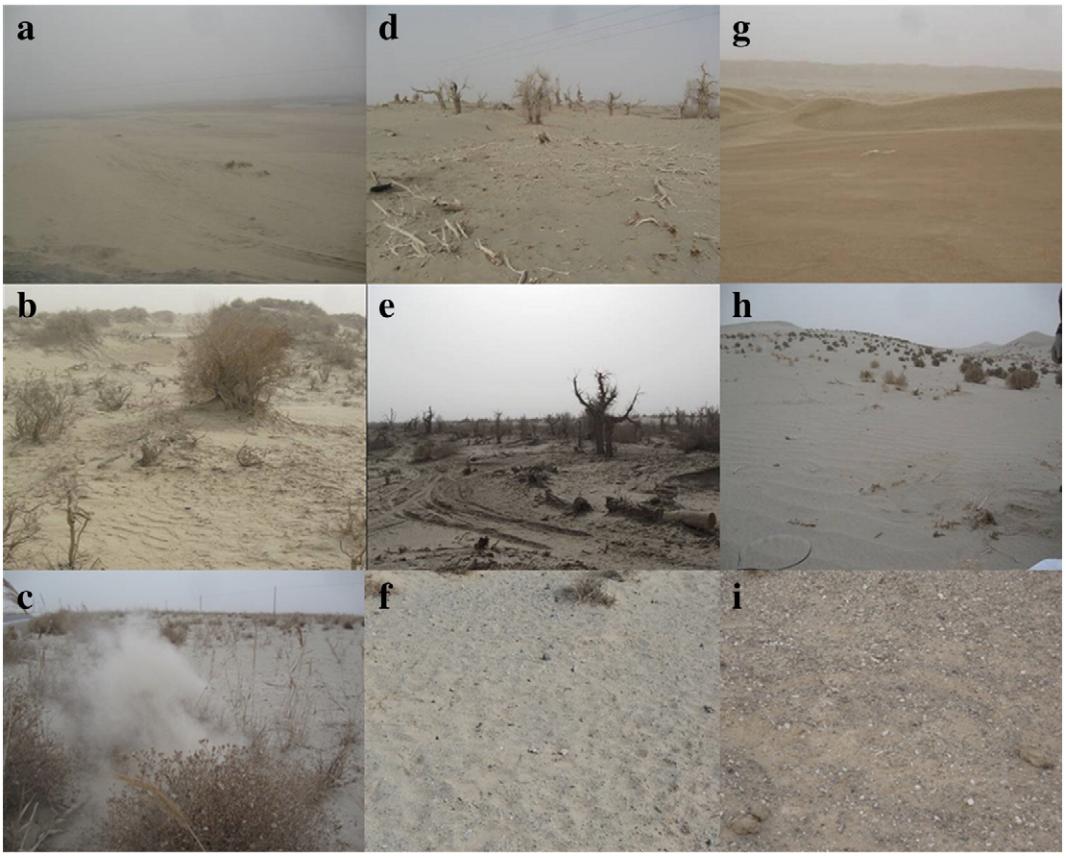

Fig. 2. Main landforms of the sampling sites. **a**) Dry Taitema Lake, **b**) Shrub dunes, **c**) Degraded reed vegetation, **d)** and **e**) Degraded diversifolia forest, **f)** and **i**) Gobi desert, **g**) Hinterland desert, **h**) Desert margin.

surface is the main dust sediment accumulation area. A localized and seasonal sand/dust storms has released an abundance of fine dust particles from the surrounding area. These have been mixed and deposited in the Taklamakan sand sea under the dominant wind force, and most particulate material are probably also reworked by the wind as the sand saltates and the dunes migrate. While dominant winds are indicated on Fig. 3, it is apparent that the winds are variable and reasonably one could conclude that these variable winds homogenize the dust in this region by remobilizing it time and again. Thus, the dust recycling that is occurring here is due to the change in seasonal wind direction.

4.2. Particle size composition of fallout dust

Grain characteristics of dust fallout not only indicate the dynamic wind environment of the monitored regions, but also show the formation processes of dust sediment. Figs. 6, 7 and 8 show curves of landscape surface dust-particle size fraction, accumulation, and grain size-standard deviation distribution for different landscape surfaces. The grain-size characteristics of dust fallout indicate that sediments contain two particle size fractions, a coarse component and fine component. Modal particle size of the coarse component in the Taklamakan sand sea surface samples was 92–143 μm, and this component represented 26.9%

Table 1
Sample descriptions (see Fig. 1 for locations).

Location	Surface classifications	Latitude and longitude	samples	Main surface characteristics	Prevailing wind direction
Eastern Desert	Desert (ML)	N 37.274°, E 82.780°; N 41.066°, E 84.243°	28	Complex dunes types with heights < 100 m	East and northeast wind
	The eastern marginal degraded land (KR)	N 41.580°, E 86.191°; N 39.085°, E 88.156°	27	Degraded Diversifolia forests, shrub dunes and Bare, flat and eroded Taitema dry lake	East and northeast wind
	The southeastern marginal Gobi and degraded land (RM)	N 38.687°, E 87.028°; N 36.807°, E 82.275°	13	Bare and eroded surfaces with high gravel content on the Gobi; Large areas of reed vegetation with varying coverage on the degraded land surfaces	East and northeast wind
Western Desert	Desert (AH)	N 37.454°, E 80.156°; N 4.366°, E 81.163°	16	Shifting dunes with sparse Diversifolia dunes and dune heights < 50 m Shifting dunes with sparse Diversifolia dunes and Diversifolia forest on the western margin desert and dune heights <50 m	Northeast, north and northwest wind
	The southwestern marginal Gobi and degraded land (MS)	N36.909°, E 80.739°; N37.707°, E 77.848°	7	Bare and eroded surfaces with high gravel content	West and northwest wind
	The northwestern marginal degraded land (SA)	N39.054°, E 77.887°; N40.406°, E 80.361°	9	Degraded Diversifolia forests and shrub dunes with many windblown sand/dust areas.	North and northwest wind

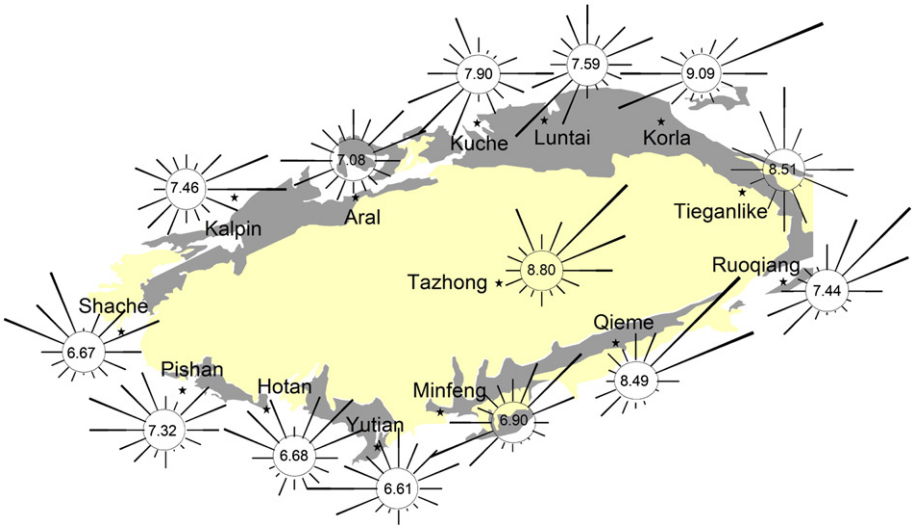

Fig. 3. Highest 10-minute mean maximum wind speed and direction of main winds during the monitoring period (5 April 2010–2 April 2011) Note: arm is average 10-min maximum wind speed from the given direction toward the central circle; values in central circle are mean maximum wind velocity ($m\ s^{-1}$).

of total sediment. Modal particle size of the fine component was 36–45 μm, representing 9.7% of total sediment. For degraded land on the desert edge and Gobi surfaces, the coarse-component modal particle size was 63–110 μm, representing 15.5–57.1% of the total sediment, whereas the fine-component modal particle size was 15–31 μm and represented 4.5–20.6%. Both the coarse and fine component modal particle sizes were larger for the sand sea and showed relatively uniform mixing, with differences in component contents not significant. In contrast, the coarse and fine component modal particle sizes were smaller and clearly different for degraded land on the desert margin and for Gobi areas. This suggests that the dust-conveying capability from the Taklamakan sand sea is much stronger than that for the Gobi and degradation surfaces on the desert edge.

For the entire study area, the curves of particle size distribution for samples collected in the two periods are consistent, with the samples separated between the coarse and fine grain-size components at 40 μm, This represents different causes of formation of the components. The modal particle size ranges are 86–106 μm and 20–40 μm (Fig. 8). The transport mode of dust particles in air suggests that particles <20 μm are transmitted from far away and that they normally exist entirely as dust. The 20-μm size is recognized as the boundary between short-term and long-term transport suspensions. Components between 20 and 70 μm are silt-sized dust material transmitted over short distances near the surface. The 70-μm size is regarded as the limit of suspended load particle size (Patterson and Gillete, 1977; Pye, 1987; Sun et al., 2000, 2002). The coarse component modal particle size range of the dust samples in our research area was 86–106 μm, larger than the critical suspended load size of 70 μm. Based on the transport mode of dust particles in air, we believe that the coarse component (>40 μm) mainly comes from local saltation during windblown sand activity. The stronger the wind energy, the larger the modal particle size of the saltation particles, and the higher the content of that coarse component. Visibly, the fine particle component (<40 μm) can be divided into remotely or locally suspended deposit components under a weak wind background. Thus, for seasonal and localized windblown sand/dust activities, the fine dust fraction (<40 μm) can be frequently recycled between the Taklamakan sand sea and active dust emission areas. Comprehensive dust fallout and its grain observation results clearly show that the fine dust particles (<40 μm) released from the active dust emission areas are easily transported and mixed

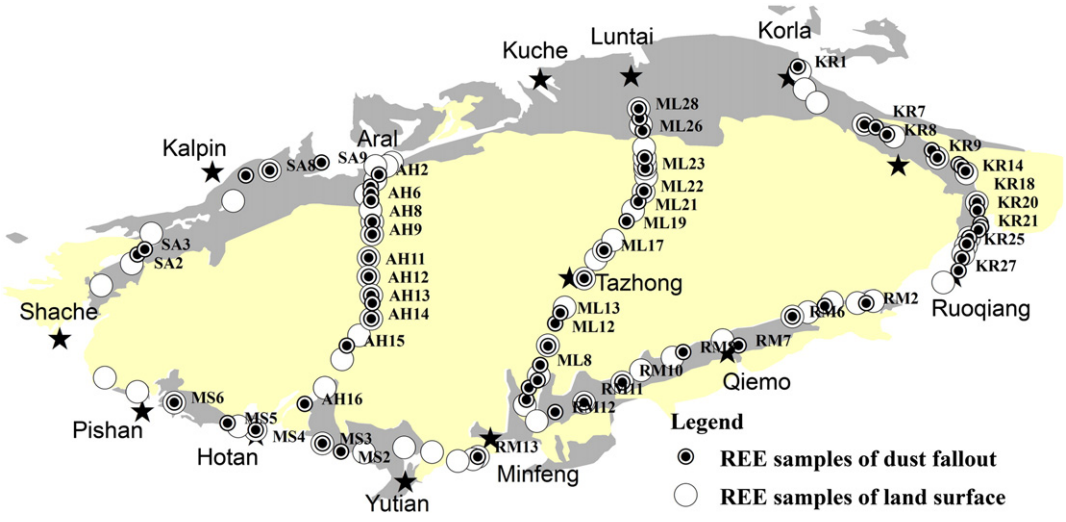

Fig. 4. Locations of monitoring sites where samples were analyzed for REE in Taklamakan Desert (Note: REE abundance data listed in Table 2).

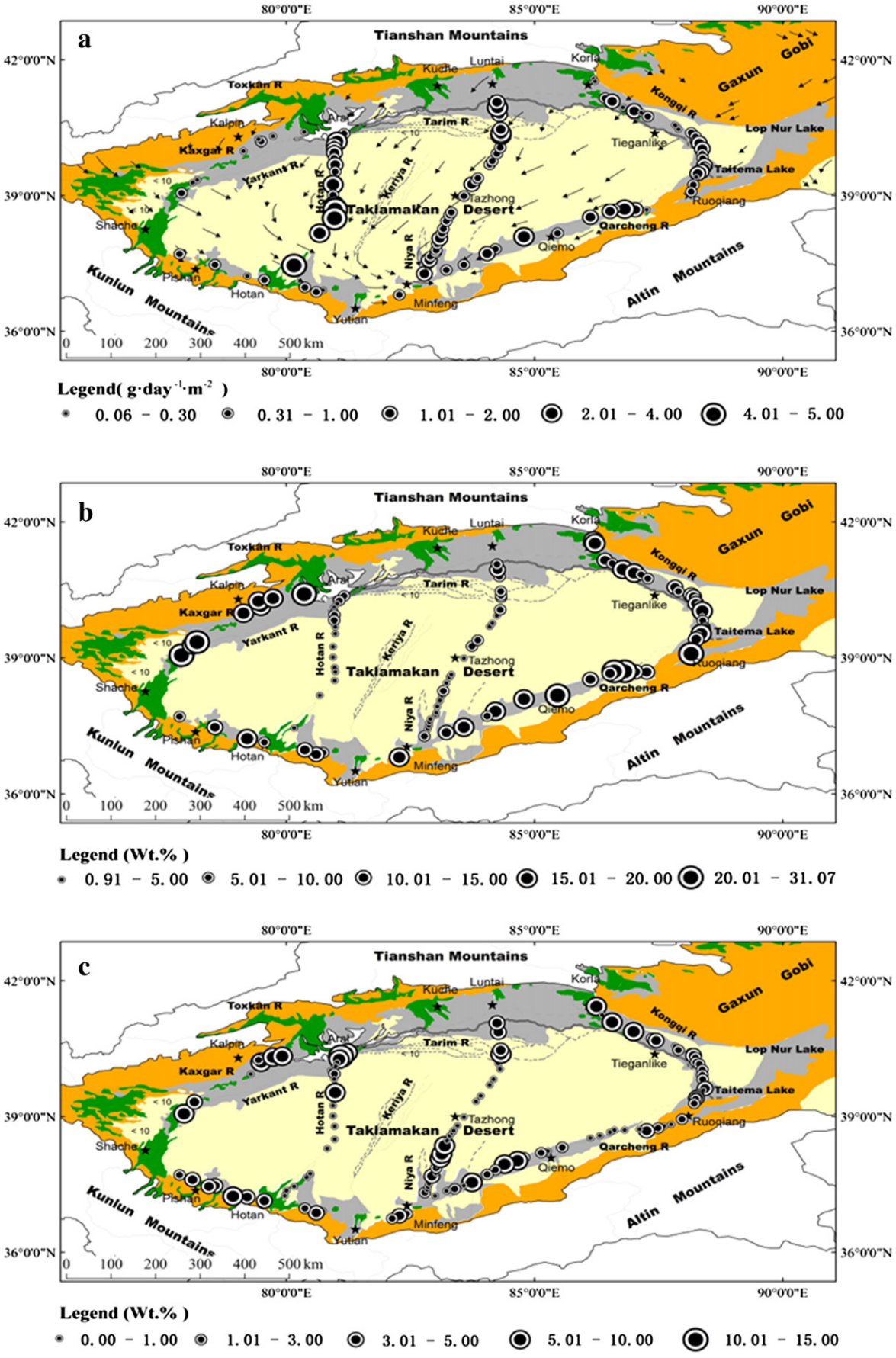

Fig. 5. Map of spatial distribution for fallout and concentrations of PM_{10} particles and their surface concentrations. **a**) The fallout of PM_{10} particles, **b**) the concentrations of PM_{10} particles in dust, and **c**) the concentrations of PM_{10} particles in the land surface sediment.

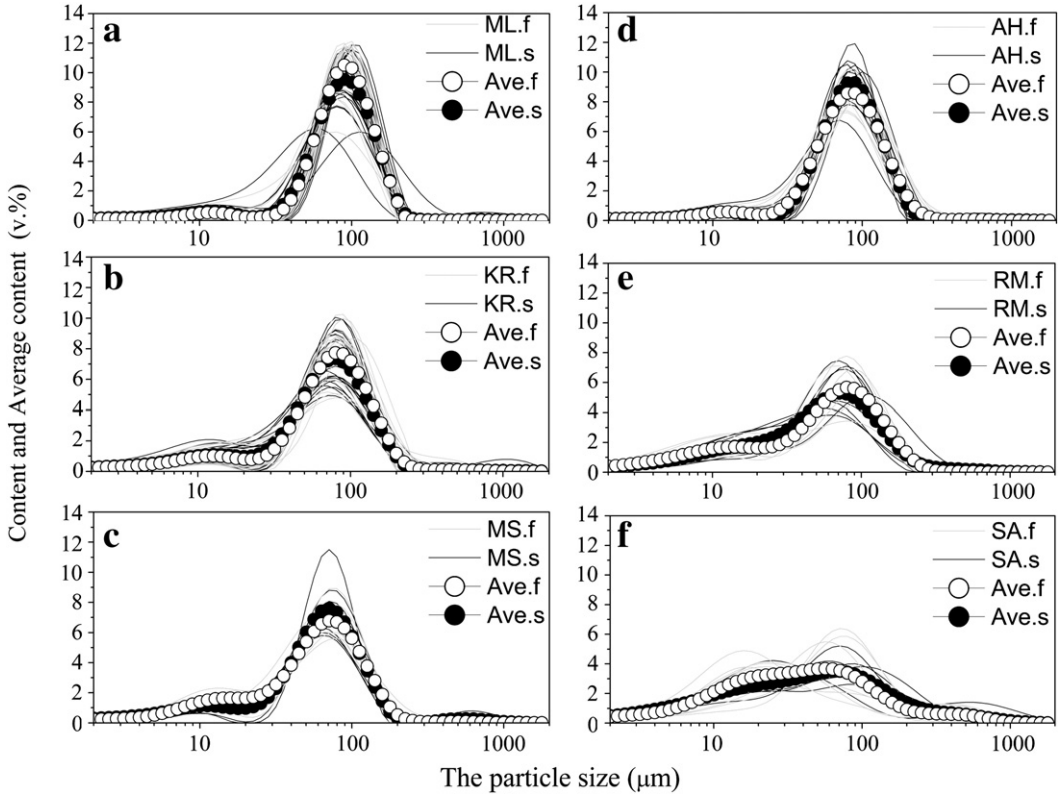

Fig. 6. Dust-particle size fraction content curves for samples from different landforms. **a**) The eastern dunes from Minfeng to Luntai (ML), **b**) the eastern margin degraded land from Koral to Ruoqiang (KR), **c**) The Gobi desert of Hotan areas (MS), **d**) the western dunes from Hotan to Aral (AH), **e**) the southeastern margin degraded land from Ruoqiang to Minfeng (RM), and **f**) the northwestern margin degraded land from Shache to Aral (SA). Note: ".f" means the first sampling period, and ".s" means the second sampling period.

in the atmosphere over the Taklamakan sand sea under prevailing wind directions, and supply abundant dust materials for the sand sea surface.

The spatial distribution of fallout and concentrations of PM10 particles for two sampling periods are shown in Fig. 9. The results show that the rates of dust deposition for most monitoring sites were approximate in the first sampling period, in fact, which mainly reflects a large-scale and strong dust-storm process. The dust fallout of the second sampling period is formed by multiple localized and seasonal sand/dust storm process and strongly influenced by dominant winds, and results show that the rates of dust deposition were significant spatial difference. Although the rate of dust fallout are significantly different for both sampling periods, in looking at the particle size data and concentrations of PM10 particles, the distributions are nearly identical for both sampling periods, suggesting that a month-long sampling is representative of the dust size distributions and compositions in study areas.

4.3. REE characteristics of PM_{10} and PM_{40-63} particles

Generally, chondrite-normalized REE patterns and REE ratios have been extensively used to indicate material provenance, since they behave conservatively and mainly transport in particulate form during earth surface processes. Eu anomalies indicating depletion or enrichment of europium relative to its neighboring REEs, are measured by Eu/Eu* ratios and calculated with the Taylor and McLennan (1985) formula $Eu/Eu^* = Eu_{CH}/[(Sm_{CH}) \times (Gd_{CH})]^{1/2}$ (subscript "$_{CH}$" indicates chondrite-normalized values). Based on REE abundance data of land surface PM_{10} fraction, dust PM_{10} and PM_{40-63} fractions listed in Table 2, chondrite-normalized patterns are depicted in Fig. 10. Eu/Eu* vs. La_{CH}/Yb_{CH} and $(La/Yb)_{CH}$ vs. La_{CH} diagrams are shown in Fig. 11. These show that chondrite-normalized REE patterns of all materials are uniform, with steep light rare earth element profiles, relatively flat heavy rare earth elements profiles and moderate Eu depletion. This indicates strongly homogeneous geochemical characteristics of dust particles in the entire Tarim Basin. However, there are great variations of REE compositions between land surface and dust fallout PM_{10} fractions, owing to sorting of grain-size distributions and heavy minerals in multiple dust recycling processes.

Figs. 10 and 11 show that the REE composition concentrations and Eu/Eu* vs. La_{CH}/Yb_{CH} and $(La/Yb)_{CH}$ vs. La_{CH} ratios of the land surface PM_{10} fraction from various regional landforms have consistent geochemical characteristics, and are significantly different in their dust fallout PM_{10} fraction. The dust fallout PM_{10} fraction from the eastern and western sand sea downstream of the prevailing wind direction has a very coherent concentration of REEs and Eu/Eu* vs. La_{CH}/Yb_{CH} and $(La/Yb)_{CH}$ vs. La_{CH} ratios, but different from the Gobi and degraded land surrounding the Taklamakan sand sea. These stark differences of REE geochemical characteristics between the land surface PM_{10} fraction from various regional landforms and dust fallout PM_{10} fraction reveal that there are two types of cycling process for fine dust particles (<40 μm) between the sand sea and the surrounding Gobi and degraded land. Multiple large-scale windblown sand/dust processes have occurred between the sand sea and the surrounding Gobi and degraded land over a long historical period. This has strongly mixed the fine fractions of the land surface sediment across the entire Tarim Basin, and geochemical characteristics manifest strong homogeneity. Localized and seasonal windblown sand/dust processes are also frequent over the entire basin, which are revealed by the different concentrations of dust fallout PM_{10} components and REE geochemical characteristics for

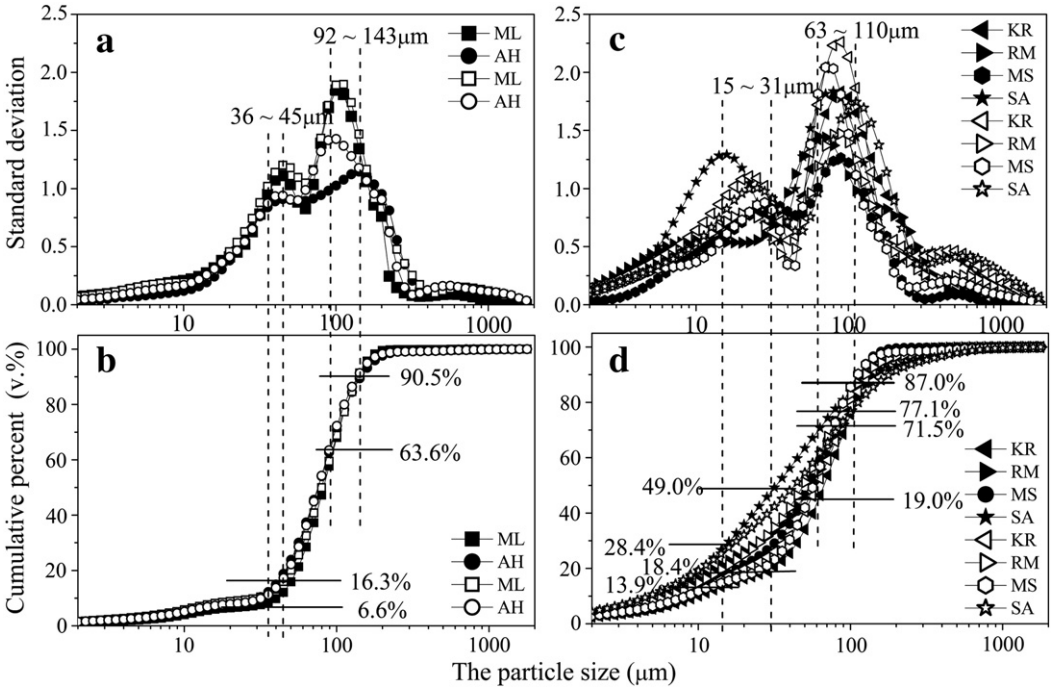

Fig. 7. Average cumulative percentage and standard deviation curves of dustfall particle fraction contents. **a)** and **b**)The dust samples from the deserts of ML and AH; **c)** and **d**) the dust samples from margin degraded land (KR, RM and SA) and Gobi desert (MS). Note: ".f" means the first sampling period, and ".s" means the second sampling period.

the various regional surfaces. Fine fraction concentrations in the peripheral area of the Taklamakan sand sea are extremely high, and large numbers of PM_{10} particles adhere to the land surface and vegetation. This readily occurs in dust events, especially with weak wind energy. However, the frequency of occurrence of these particles varies, because of dust content differences between surface types and in response to variable wind energy. Thus, the sampled deposits appear to have been collected from areas with multiple dust sedimentation processes. This has led to very different concentrations of PM_{10} components and their REE geochemical characteristics in dust fallout on various regional surfaces.

The results also show that REE concentrations and Eu/Eu* vs. La_{CH}/Yb_{CH} and $(La/Yb)_{CH}$ vs. La_{CH} ratios of dust PM_{10} fraction from the sand sea downwind are very homogeneous, and that REE concentrations are generally much higher than in degraded areas on the desert edge and Gobi surfaces under the path of the dominant wind. Usually, heavy minerals reside mostly in fine fractions and may significantly affect REE patterns of the sediments (Taylor and McLennan, 1985). It has been shown that heavy minerals can be selectively sorted in high-energy wind regimes that separate the fine-grained heavy minerals from coarse quartz and feldspar (Komar and Wang, 1984; Abuodha, 2003). The greatest sand-drift intensity and highest frequency of sand-dust storms occur between the Taklamakan sand sea and the surrounding Gobi and degraded land (Shao et al., 2002; Zu et al., 2008). This may contribute to transport of the PM_{10} fraction from the very fine-grained sediment and heavy mineral assemblages in the sand sea. This may contribute to the substantial accumulation of PM_{10} and to REE concentrations in dust fallout on desert surfaces. Thus, dust formation on the modern desert surfaces is closely correlated with dust emission from wind erosion on the desert edge, Gobi and degraded surfaces.

Compelled by the dust PM_{10} fraction, the REE concentrations and Eu/Eu* vs. La_{CH}/Yb_{CH} diagram and $(La/Yb)_{CH}$ vs. La_{CH} ratios of PM_{40-63} have a spatial distribution difference between the eastern and western sand sea. This suggests that the PM_{40-63} fraction does not fully mix between those two areas during the dust deposition process. The process in the eastern sand sea is mainly controlled by strong northeasterly airflows, whereas westerly, northwesterly and northerly airflows affect the western sand sea. Wang et al. (2012) showed that trace element concentrations of the silt and clay fraction of the land surface sediments clearly varied between the western and eastern sand sea; the former had high concentrations, and the latter low ones. Fig. 11 and Table 2 show that a trend is apparent between ML (eastern dunes from Minfeng to Luntai) and AH (western dunes), where AH

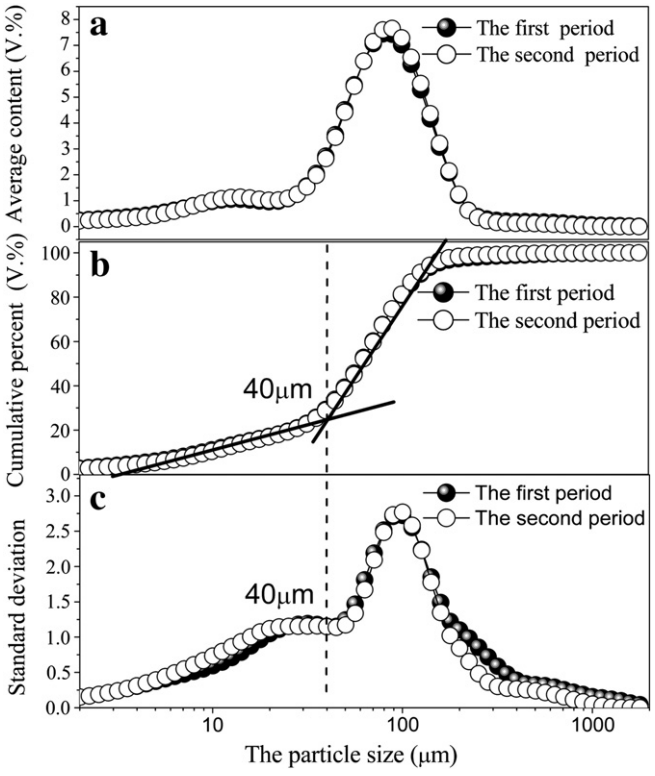

Fig. 8. Cumulative percentage and standard deviation curves of dustfall particle fraction contents for entire samples. **a**) Average percentage content of dustfall particle fraction contents, **b**) average cumulative percentage of dustfall particle fraction contents, and **c**) the standard deviation of all dustfall particles fraction contents.

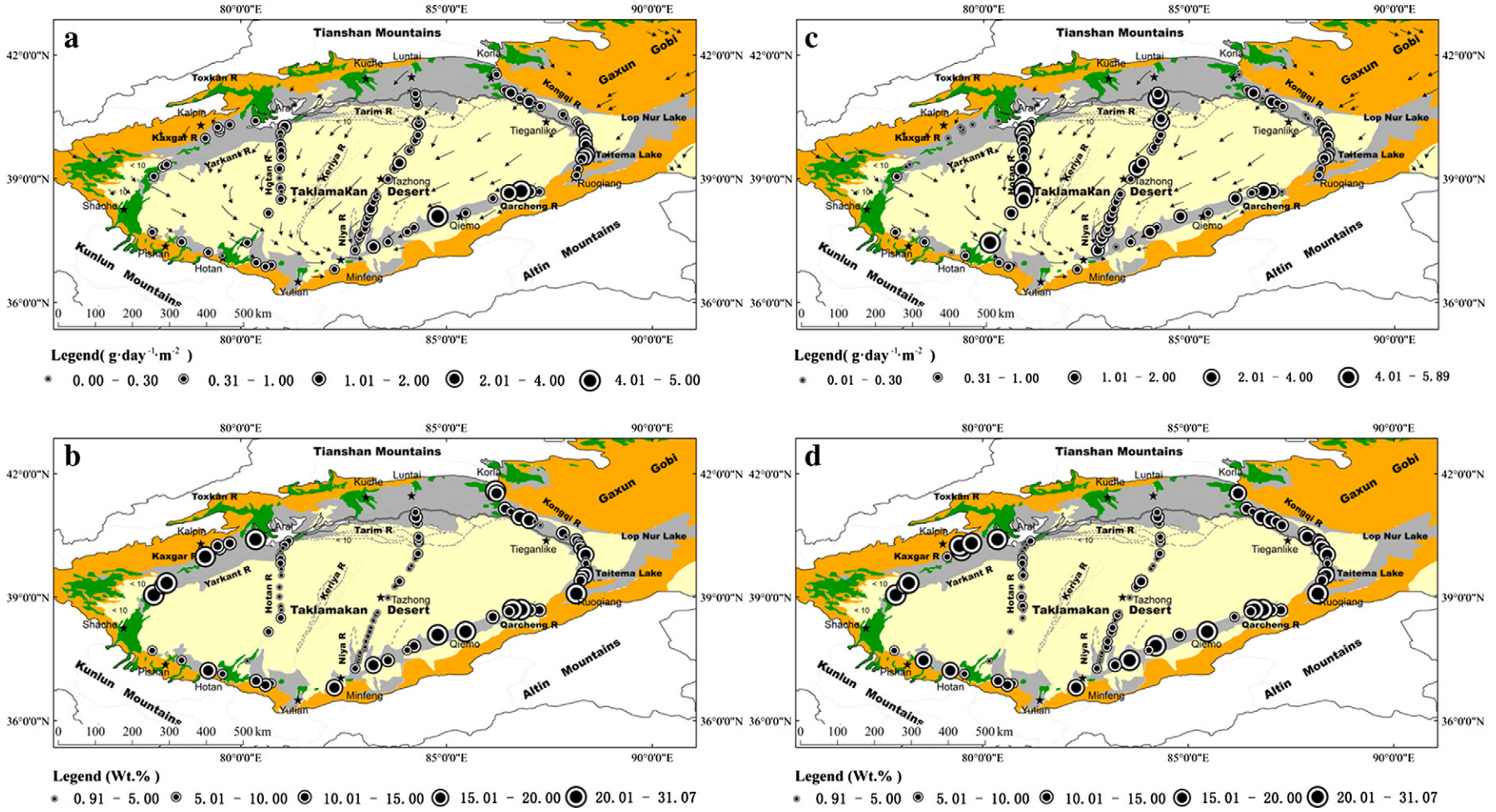

Fig. 9. Map of spatial distribution of fallout and concentrations of PM_{10} particles for two sampling periods. **a**) The fallout of PM_{10} particles for the first sampling period, **b**) the concentrations of PM_{10} particles in the dust for the first sampling period, **c**) the fallout of PM_{10} particles for the second sampling period, **and d**) the concentrations of PM_{10} particles in the dust for the second sampling period.

Table 2
REE concentrations (mg/kg) in different materials and grain sizes from the Taklamakan Desert and surrounding areas. *n* is the sample number.

	La	Ce	Pr	Nd	Sm	Eu	Gd	Tb	Dy	Ho	Er	Tm	Yb	Lu	Y	$(La/Yb)_{CH}/La_{CH}$	$(La/Yb)_{CH}/(Eu/Eu^*)_{CH}$
ML1 ($n = 17$)	39.88	73.87	8.98	33.81	6.57	1.24	5.48	1.01	5.18	0.92	2.78	0.46	3.03	0.45	27.35	0.084	14.49
AH1 ($n = 13$)	45.55	86.14	10.18	39.09	7.53	1.33	6.07	1.10	5.49	0.97	2.94	0.48	3.17	0.47	28.86	0.080	16.41
KR1 ($n = 18$)	31.89	59.46	7.11	27.58	5.34	1.11	4.44	0.84	4.36	0.80	2.40	0.40	2.60	0.39	23.44	0.097	12.32
RM1 ($n = 9$)	35.06	65.99	7.91	30.60	5.94	1.18	5.00	0.94	4.86	0.88	2.66	0.44	2.86	0.43	26.14	0.088	12.90
MS1 ($n = 5$)	40.24	76.36	9.03	34.64	6.68	1.24	5.49	1.01	5.06	0.90	2.73	0.44	2.91	0.43	26.48	0.088	15.28
SA1 ($n = 5$)	29.02	54.50	6.48	25.12	4.85	1.02	4.01	0.75	3.92	0.71	2.14	0.35	2.31	0.34	21.06	0.109	12.39
Average values	**36.94**	**69.39**	**8.28**	**31.81**	**6.15**	**1.19**	**5.08**	**0.94**	**4.81**	**0.86**	**2.61**	**0.43**	**2.81**	**0.42**	**25.56**	**0.091**	**13.96**
ML2 ($n = 20$)	30.34	56.04	6.87	26.34	4.97	1.05	4.14	0.79	4.06	0.73	2.18	0.36	2.35	0.35	21.16	0.108	12.63
AH2 ($n = 19$)	42.15	77.67	9.41	35.94	6.86	1.27	5.74	1.05	5.31	0.95	2.86	0.47	3.03	0.45	28.12	0.084	15.63
KR2 ($n = 11$)	27.76	51.01	6.24	24.01	4.58	1.00	3.87	0.74	3.79	0.69	2.05	0.34	2.22	0.33	20.41	0.115	11.99
RM2 ($n = 12$)	29.33	54.93	6.73	25.71	4.84	1.01	3.97	0.76	3.86	0.69	2.05	0.34	2.19	0.32	20.02	0.115	13.25
MS2 ($n = 12$)	29.70	54.44	6.65	25.74	4.97	1.05	4.16	0.81	4.26	0.78	2.34	0.39	2.50	0.37	23.02	0.101	11.72
SA2 ($n = 5$)	26.80	49.02	5.93	23.00	4.43	0.95	3.73	0.71	3.66	0.67	1.99	0.33	2.14	0.32	19.74	0.118	12.17
Average values	**31.01**	**57.18**	**6.97**	**26.79**	**5.11**	**1.06**	**4.27**	**0.81**	**4.16**	**0.75**	**2.25**	**0.37**	**2.41**	**0.36**	**22.08**	**0.107**	**12.90**
ML3 ($n = 16$)	32.59	66.38	7.40	28.33	5.34	1.14	4.44	0.87	4.79	0.90	2.75	0.47	3.12	0.48	25.41	0.081	10.17
AH3 ($n = 13$)	34.84	76.85	7.97	30.55	5.77	1.19	4.81	0.93	5.00	0.93	2.84	0.49	3.24	0.50	25.99	0.078	10.89
KR3 ($n = 17$)	32.23	62.79	7.31	28.04	5.25	1.10	4.33	0.83	4.47	0.83	2.49	0.42	2.75	0.42	23.25	0.092	11.59
RM3 ($n = 9$)	34.61	67.55	7.91	30.50	5.72	1.18	4.65	0.89	4.68	0.86	2.58	0.43	2.82	0.43	24.06	0.089	12.25
MS3 ($n = 5$)	31.45	62.70	7.20	27.66	5.20	1.10	4.27	0.83	4.57	0.86	2.59	0.43	2.86	0.43	23.60	0.089	10.81
SA3 ($n = 5$)	32.06	61.92	7.30	27.94	5.22	1.13	4.30	0.82	4.34	0.80	2.42	0.40	2.65	0.40	22.38	0.095	11.51
Average values	**32.96**	**66.36**	**7.52**	**28.84**	**5.42**	**1.14**	**4.47**	**0.86**	**4.64**	**0.86**	**2.61**	**0.44**	**2.91**	**0.44**	**24.12**	**0.087**	**11.20**

♦.1: Dust fallout PM10 composition samples.
♦.2: Dust fallout PM40-63composition samples.
♦.3: Land surface PM10 composition samples.

becomes enriched in REE, we think because of fractionation/sorting of minerals by the wind among the dunes. There is no clear sorting among the other samples, but complete overlap, likely because these sediments don't travel nearly as far—potentially due to roughness of the surface along the desert margin. These results further suggests that the coarse fraction (>40 μm) of dust fallout is mainly affected by the locally dominant wind and sediment province of particular land surfaces.

The test results of REE for PM_{10} and $PM_{40–63}$ particles show that under the dominant wind force, abundant fine dust particles released from the surrounding area supplies substantial dust material for the Taklamakan sand sea surface in seasonal and localized windblown sand/dust processes, and also provide for storage of abundant amounts of the fine dust fraction, representing a potential future source for large-scale dust processes.

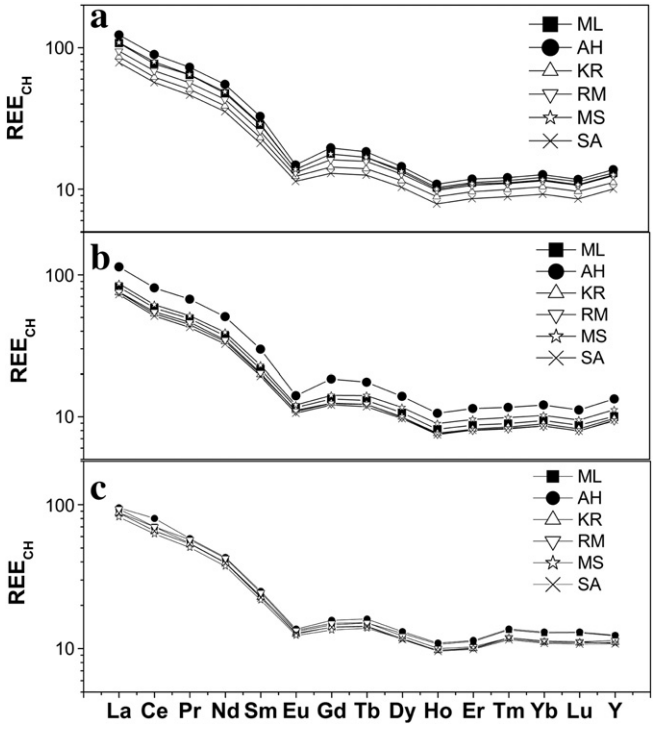

Fig. 10. Chondrite-normalized REE diagram (subscript "CH" indicates chondrite-normalized values) of land surface PM_{10}, and dust PM_{10} and $PM_{40–63}$ fractions from different landforms. **a**) PM_{10} fraction of dustfall, **b**) $PM_{40–63}$ fraction of dustfall, and **c**) PM_{10} fraction of land surface.

5. Conclusions

As a large source of global dust production, dust-forming processes of the modern Taklamakan sand sea surface are closely correlated with dust released from active dust site sources in surrounding areas, such as dry lakes and riverbeds, oases via degradation, and Gobi surfaces.

The monitoring results of dust fallout and its particle size suggest that the Taklamakan sand sea is surrounded by dust sources. This means that as a unique landform body under the influence of the dominant wind force, it is an important dust deposit area. A localized and seasonal sand/dust storm has released an abundance of fine dust particles from the surrounding area. These have been mixed and deposited in the Taklamakan sand sea under the dominant wind force, and most particulate material are probably also reworked by the wind as the sand saltates and the dunes migrate. These variable winds homogenize the dust in this region by remobilizing it time and again. Thus, the dust recycling that is occurring here is due to the change in the seasonal wind direction.

Generally speaking, the dust-conveying potential of the Taklamakan sand sea is much stronger than that of the Gobi and degradation surfaces on the desert edge. The fine dust fraction (<40 μm) can be frequently recycled between the sand sea and active dust emission areas during seasonal and localized sand/dust activit. Chondrite-normalized REE patterns and Eu/Eu* vs. La CH/Yb CH and (La/Yb)CH vs. LaCH ratios of land surface and dust PM10 fractions further suggest that under the dominant wind force, abundant fine dust particles released from the surrounding area supply abundant fine particles for dust formation of the Taklamakan sand sea surface during seasonal and localized windblown sand/dust activities, and also provide for storage of abundant

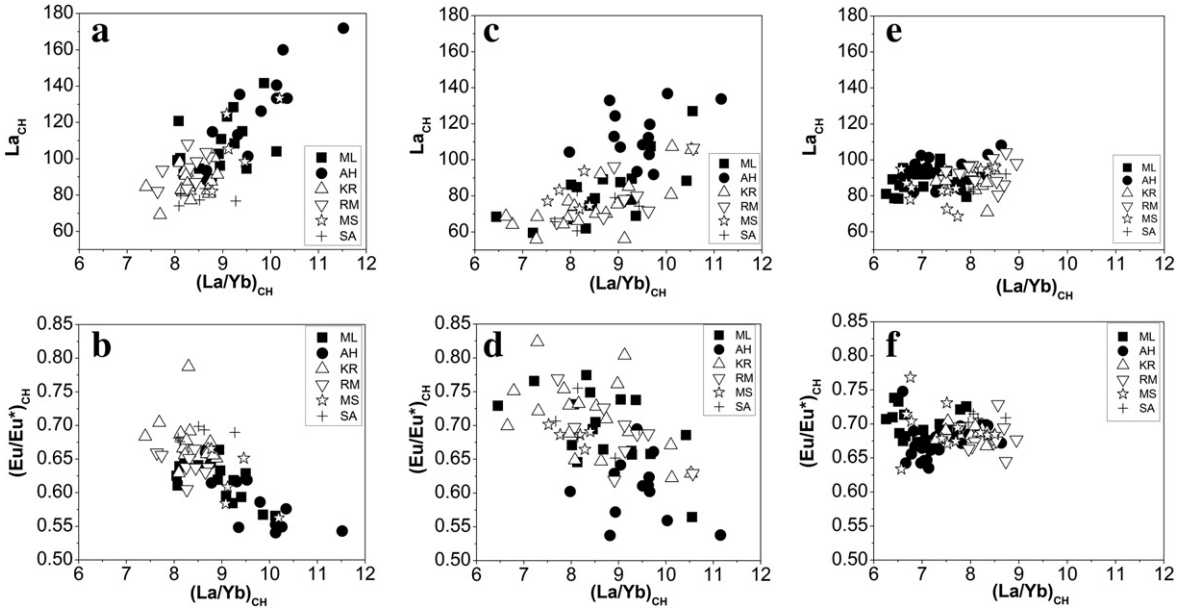

Fig. 11. Eu/Eu* vs. La_{CH}/Yb_{CH} and $(La/Yb)_{CH}$ vs. La_{CH} diagrams of surface PM_{10}, and dust PM_{10} and PM_{40-63} fractions from different landforms. **a)** and **b**) PM_{10} fraction of dustfall, **c** and **d**) PM40-63 fraction of dustfall, and **e)** and **f**) PM_{10} fraction of land surface.

amounts of the fine dust fraction, representing a potential future source for large-scale dust processes.

Acknowledgments

This work was supported by the Desert Surface Processes and Mechanisms Program of the Hundred Talents Project of the Chinese Academy of Sciences and the Natural Science Foundation of China (41201001), and the Foundation for Excellent Youth Scholars of CAREERI, CAS (No. 51Y251B31).

References

Abuodha, J.O.Z., 2003. Grain size distribution and composition of modern dune and beach sediments, Malindi Bay coast. Kenya. J. Afr. Earth. Sci. 36, 41–54.
Amit, R., Enzel, Y., Mushkin, A., Gillespie, A., Batbaatar, J., Crouvi, O., Vandenberghe, J., An, Z., 2014. Linking coarse silt production in Asian sand deserts and Quaternary accretion of the Chinese Loess Plateau. Geology 42, 23–26.
Crouvi, O., Amit, R., Enzel, Y., Porat, N., Sandler, A., 2008. Sand dunes as major proximal dust source for late Pleistocene loess in the Negev Desert, Israel. Quat. Res. 70, 275–282.
Crouvi, O., Schepanski, K., Amit, R., Gillespie, A.R., Enzel, Y., 2012. Multiple dust sources in the Sahara Desert: the importance of sand dunes. Geophys. Res. Lett. 39. http://dx.doi.org/10.1029/2012GL052145.
Gao, H., Washington, R., 2009. The spatial and temporal characteristics of TOMS AI over the Tarim Basin, China. Atmos. Environ. 43, 1106–1115.
Gao, H., Washington, R., 2010a. Transport trajectories of dust originating from the Tarim Basin, China. Int. J. Climatol. 30, 291–304.
Gao, H., Washington, R., 2010b. Arctic oscillation and the inter-annual variability of dust emissions from the Tarim Basin: a TOMS AI based study. Clim. Dyn. 35, 511–522.
Komar, R.O., Wang, C., 1984. Processes of selective grain transport and the formation of placers on beaches. J. Geol. 92, 637–655.
Laurent, B., Marticorena, B., Bergametti, G., Mei, F., 2006. Modeling mineral dust emissions from Chinese and Mongolian deserts. Global Planet. Change 52 (1–4), 121–141.
Li, S.K., Lu, M., Wang, K.R., Wang, X., 2008. Soil erosion of the main ground surface types influences on formation of dust storm in South Xinjiang. Sci. Agric. Sin. 41 (10), 3158–3167 (in chinese).
Patterson, E.M., Gillete, D.A., 1977. Commonalities in measured size distribution for aerosols having a soil-derived component [J]. J. Geophys. Res. 82, 2074–2082.
Prospero, J.M., Gignoux, P., Torres, O., Nicholson, S.E., Gill, T.E., 2002. Environmental characterization of global sources of atmospheric soil dust identified with the Nimbus 7 Total Ozone Mapping Spectrometer (TOMS) absorbing aerosol product. Rev. Geophys. 40.
Pye, K., 1987. Aeolian Dust and Dust Deposits. Academic Press, London p. 334.
Shao, Y., Jung, E., Leslie, L.M., 2002. Numerical predictions of northeast Asian dust storms using an integrated wind erosion modelling system. J. Geophys. Res. 107, 4814–4837. http://dx.doi.org/10.1029/2001JD001493.
Shao, Y., et al., 2003. Northeast Asian dust storms: Real-time numerical prediction and validation. J. Geophys. Res. 108, 4691–4709. http://dx.doi.org/10.1029/2003JD003667.
Sun, D.H., Lu, H.Y., David, R., Sun, Y.B., Wu, S.G., 2000. Bimode Grain-size distribution of Chinese loess and its paleoclimate implication. Sedimentol. Sin. 18 (3), 327–335 (in chinese).
Sun, D.H., Bloemendal, J., Rea, D.K., 2002. Grain size distribution of function of polymodal sediments in hydraulic and Aeolian environments and numerical partitioning of the sedimentary components. Sed. Geol. 152, 263–277.
Ta, W.Q., Dong, Z.B., 2006. Effect of the 1950s large-scale migration for land reclamation on spring dust storms in Northwest China. Atmos. Environ. 40, 5815–5823.
Ta, W.Q., Wang, H.B., Jia, X.P., 2013. External supply of dust regulates dust emissions from sand deserts. Catena 110, 113–118.
Taylor, S.R., McLennan, S.M., 1985. The Continental Crust: Its Composition and Evolution. Blackwell, Oxford.
Tegen, I., 2003. Modeling the mineral dust aerosol cycle in the climate system. Quat. Sci. Rev. 22, 1821–1834.
Tegen, I., Harrison, S.P., Kohfeld, K., Prentice, I.C., Coe, M., Heimann, M., 2002. Impact of vegetation and preferential source areas on global dust aerosol: results from a model study. J. Geophys. Res. 107 (D21), 4576.
Teresa, M., Xavier, Q., Sonia, C.o, Alastuey, A., Emilio, C., Herrmann, Ludger, Mounkaila, Mohammed, Elvira, Josep, Gibbons, Wes, 2006. Geochemical variations in aeolian mineral particles from the Sahara–Sahel Dust Corridor. Chemosphere 65, 261–270.
Wang, H.B., Jia, X.P., 2012. Field observation of windblown sand dust in the Takimakan Desert, NW China, and insights into modern dust sources. Land Degrad. Dev. http://dx.doi.org/10.1002/idr.1129.
Wang, X., Xia, D., Wang, T., Xie, X., Li, J., 2008. Dust sources in arid and semiarid China and southern Mongolia: impacts of geomorphologic setting and surface materials. Geomorphology 97, 583–600.
Wang, X.m, Dong, Z.B., Zhang, C.X., Qian, G.Q., Luo, W.Y., 2009. Characterization of the composition of dust fallout and identification of dust sources in arid and semiarid North China. Geomorphology 112, 144–157.
Wang, X., Zhang, C.X., Wang, H.T., Qian, G.Q., Luo, W.Y., Lu, J.F., Wang, L., 2011. The significance of Gobi desert surfaces for dust emissions in China: an experimental study. Environ. Earth Sci. 64, 1039–1050.
Wang, H.B., Jia, X.P., Xiao, J.H., Shi, X.M., 2012. Provenance and geochemical characteristics of the silt and clay fraction in the Taklamakan Desert, Northwestern China. Arid Land Res. Manag. 26, 85–1022.
Washington, R., Todd, M.C., Lizcano, G., Tegen, I., Flamant, C., Koren, I., Gignoux, P., Engelstaedter, S., Bristow, C.S., Zender, C.S., Goudie, A.S., Warren, A., Prospero, J.M., 2006. Links between topography, wind, deflation, lakes and dust: the case for the Bodele depression, Chad. Geophys. Res. Lett. 33.
Xie, Y.Y., Liang, Peng, Meng, J., He, K., Zang, S.y, 2009. Obtainment of grain-size populations sensitive to material source area of sand-dust fallouts in Harbin City and their source analysis. Geogr. Geo-Inf. Sci. 25 (6), 51–55 (in chinese).
Yang, X., 2001. The oases along the Keriya River in the Taklamakan Desert, China, and their evolution since end of last glaciation. Environ. Geol. 41, 314–320.

Yang, X., Zhu, Z., Jaekel, D., Owen, L., Han, J., 2002. Late Quaternary palaeoenvironment change and landscape evolution along the Keriya River, Xinjiang, China: the relationship between high mountain glaciation and landscape evolution in foreland desert regions. Quat. Int. 97 (98), 155–166.
Yang, X., Preusser, F., Radtke, U., 2006a. Late Quaternary environmental changes in the Taklamakan Desert, western China, inferred from OSL-dated lacustrine and aeolian deposits. Quat.Sci. Rev. 25, 923–932.
Yang, X., Liu, Z., Zhang, F., White, P., Wang, X., 2006b. Hydrological changes and land degradation in the southern and eastern Tarim Basin, Xinjiang, China. Land Degrad. Dev. 17, 381–392.
Yang, X.P., Zhu, B.Q., White, P.D., 2007. Provenance of aeolian sediment in the Taklamakan Desert of western China, inferred from REE and major-elemental data. Quat. Int. 175, 71–85.
Yang, X., Scuderi, L., Paillou, P., Liu, Z., Li, H., Ren, X., 2011. Quaternary environmental changes in the drylands of China—a critical review. Quat. Sci. Rev. 30, 3219–3233.
Yang, X., Li, H., Conacher, A., 2012. Large-scale controls on the development of sand seas in northern China. Quat. Int. 250, 74–83.
Zhang, X., Zhang, G., Zhu, G., Zhang, D., An, Z., Chen, T., Huang, X., 1996. Elemental tracers for Chinese source dust. Sci. China, Ser. D Earth Sci. 39, 512–521.
Zhang, X., Arimoto, R., Zhu, G., Chen, T., Zhang, G., 1998. Concentration, size-distribution and deposition of mineral aerosol over Chinese desert regions. Tellus 50B, 317–330.
Zhang, X.Y., Gong, S.L., Zhao, T.L., Arimoto, R., Wang, Y.Q., Zhou, Z.J., 2003a. Sources of Asian dust and role of climate change versus desertification in Asian dust emission. Geophys. Res. Lett. 30, 2272. http://dx.doi.org/10.1029/2003GL018206.
Zhang, X.Y., Gong, S.L., Zhao, T.L., Arimoto, R., Wang, Y.Q., Zhou, Z.J., 2003b. Sources of Asian dust and role of climate change versus desertification in Asian dust emission. Geophys. Res. Lett. 30, 2272. http://dx.doi.org/10.1029/2003GL018206.
Zhu, Z., Chen, Z., Wu, Z., Li, B., Wu, G., 1981. Study on the Geomorphology ofWind-Drift Sands in the Taklimakan Desert. Science Press: Beijing (3), 110 (in Chinese).
Zu, R.P., Xue, X., Qiang, M.R., Yang, B., Qu, J.J., Zhang, K.C., 2008. Characteristics of near-surface wind regimes in the Taklimakan Desert. China. Geomorphology 96, 39–47.
Zhang, Q.G., Kang, S.C., Kaspari, S., Li, C.L., Qin, D.H., Mayewski, P.A., Hou, S., 2009. Rare earth elements in an ice core from Mt. Everest: seasonal variations and potential sources. Atmos. Res. 94, 300–312.